Defense Nuclear Agency
Alexandria, VA 22310-3398

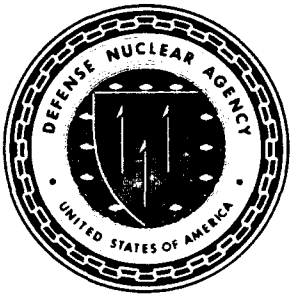

DNA-TR-89-55

Plasma Cloud Behavior

Lewis M. Linson
Science Applications International Corporation
10260 Campus Point Drive
San Diego, CA 92121

August 1991

Technical Report

CONTRACT No. DNA 001-80-C-0246

Destroy this report when it is no longer needed. Do not return to sender.

PLEASE NOTIFY THE DEFENSE NUCLEAR AGENCY, ATTN: CSTI, 6801 TELEGRAPH ROAD, ALEXANDRIA, VA 22310-3398, IF YOUR ADDRESS IS INCORRECT, IF YOU WISH IT DELETED FROM THE DISTRIBUTION LIST, OR IF THE ADDRESSEE IS NO LONGER EMPLOYED BY YOUR ORGANIZATION.

DISTRIBUTION LIST UPDATE

This mailer is provided to enable DNA to maintain current distribution lists for reports. We would appreciate your providing the requested information.

☐ Add the individual listed to your distribution list.

☐ Delete the cited organization/individual.

☐ Change of address.

NOTE:
Please return the mailing label from the document so that any additions, changes, corrections or deletions can be made more easily.

NAME: _____

ORGANIZATION: _____

OLD ADDRESS	CURRENT ADDRESS
_____	_____
_____	_____
_____	_____

TELEPHONE NUMBER: ( ) _____

SUBJECT AREA(s) OF INTEREST:

_____	_____
_____	_____
_____	_____

DNA OR OTHER GOVERNMENT CONTRACT NUMBER: _____

CERTIFICATION OF NEED-TO-KNOW BY GOVERNMENT SPONSOR (if other than DNA):

SPONSORING ORGANIZATION: _____

CONTRACTING OFFICER OR REPRESENTATIVE: _____

SIGNATURE: _____

CUT HERE AND RETURN

Director
Defense Nuclear Agency
ATTN: TITL
Washington, DC 20305-1000

Director
Defense Nuclear Agency
ATTN: TITL
Washington, DC 20305-1000

REPORT DOCUMENTATION PAGE

Form Approved OMB No. 0704-0188

1. AGENCY USE ONLY (Leave blank)	2. REPORT DATE	3. REPORT TYPE AND DATES COVERED
	910801	Technical 800701 - 830201

4. TITLE AND SUBTITLE

Plasma Cloud Behavior

5. FUNDING NUMBERS

C - DNA 001-80-C-0246
PE - 62715H
PR - I25AAXH
TA - X
WU - DH004849

6. AUTHOR(S)

Lewis M. Linson

7. PERFORMING ORGANIZATION NAME(S) AND ADDRESS(ES)

Science Applications International Corporation
10260 Campus Point Drive
San Diego, CA 92121

8. PERFORMING ORGANIZATION REPORT NUMBER

SAIC-89/1097

9. SPONSORING/MONITORING AGENCY NAME(S) AND ADDRESS(ES)

Defense Nuclear Agency
6801 Telegraph Road
Alexandria, VA 22310-3398
RAAE/Wittwer

10. SPONSORING/MONITORING AGENCY REPORT NUMBER

DNA-TR-89-55

11. SUPPLEMENTARY NOTES

This work was sponsored by the Defense Nuclear Agency under RDT&E RMSS Code B322080462 I25AAXHX64214 H2590D.

12a. DISTRIBUTION/AVAILABILITY STATEMENT

Approved for public release; distribution is unlimited.

12b. DISTRIBUTION CODE

13. ABSTRACT *(Maximum 200 words)*

Participation in the DNA-sponsored PLACES (Position Location And Communications Effects Simulations) and Midnight Sky field operations is described. In the former, four barium releases were made during the period 4 to 12 December 1980 from Eglin AFB, Florida. The range of velocities experienced was greater than before at this location. The principal challenge was to perform real-time tracking of the ion cloud so as to predict a future aim point for use in targeting beacon and probe rockets. Recommendations for obtaining smoother tracking data involve determining the motion of a field line through the ion cloud rather than an indeterminate point in the cloud, making measurements at set intervals, and coordinating measurements by more than one observer. During Midnight Sky, 2 barium releases were made on 29 March 81 and 2 April 81. The first went westerly at 450 m/s while the second was nearly motionless. A small aircraft was positioned so as to take photographs up the magnetic field line during the second release. It is strongly urged that a complete dry run including all participants, communications links, and necessary operations be carried out before a test event.

14. SUBJECT TERMS		15. NUMBER OF PAGES
PLACES	Plasma Clouds	48
Midnight Sky	Striations	16. PRICE CODE
Barium Releases	Ionospheric Plasmas	

17. SECURITY CLASSIFICATION OF REPORT	18. SECURITY CLASSIFICATION OF THIS PAGE	19. SECURITY CLASSIFICATION OF ABSTRACT	20. LIMITATION OF ABSTRACT
UNCLASSIFIED	UNCLASSIFIED	UNCLASSIFIED	SAR

CLASSIFIED BY:

N/A since Unclassified

DECLASSIFY ON:

N/A since Unclassified

PREFACE

The analyses carried out in this report have benefitted from many useful discussions with Dr. C. W. Prettie of BRA, Major Leon A. Wittwer of DNA, and Dr. S. T. Zalesak of NRL. The author would like to express his appreciation to Ms. E. A. Greene for her assistance in the data analysis and for upgrading and documenting the PROJCT code. Special thanks are due to Mr. W. P. Boquist of Technology International Corporation for his hospitality and cooperation in providing access to his original film and data records and providing copies of selected data.

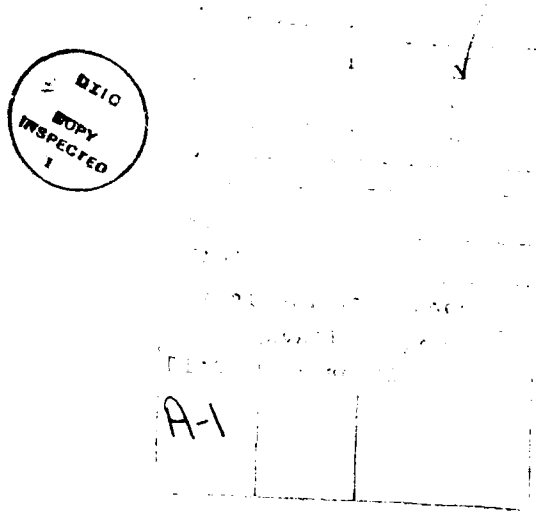

CONVERSION TABLE

Conversion factors for U.S. Customary to metric (SI) units of measurement

MULTIPLY → TO GET	BY	TO GET ← DIVIDE
angstrom	1.000 000 X E -10	meters (m)
atmosphere (normal)	1.013 25 X E +2	kilo pascal (kPa)
bar	1.000 000 X E + 2	kilo pascal (kPa)
barn	1.000 000 X E -28	meter^2 (m^2)
British thermal unit (thermochemical)	1.054 350 X E + 3	joule (J)
calorie (thermochemical)	4.184 000	joule (J)
cal (thermochemical)/cm^2	4.184 000 X E -2	mega joule/m^2 (MJ/m^2)
curie	3.700 000 X E +1	*giga becquerel (GBq)
degree (angle)	1.745 329 X E -2	radian (rad)
degree Fahrenheit	t_k = (t°F + 459.67)/1.8	degree kelvin (K)
electron volt	1.602 19 X E -19	joule (J)
erg	1.000 000 X E -7	joule (J)
erg/second	1.000 000 X E -7	watt (W)
foot	3.048 000 X E -1	meter (m)
foot-pound-force	1.355 818	joule (J)
gallon (U.S. liquid)	3.785 412 X E -3	meter^3 (m^3)
inch	2.540 000 X E -2	meter (m)
jerk	1.000 000 X E +9	joule (J)
joule/kilogram (J/kg)(radiation dose absorbed)	1.000 000	Gray (Gy)
kilotons	4.183	terajoules
kip (1000 lbf)	4.448 222 X E +3	newton (N)
kip/inch^2 (ksi)	6.894 757 X E +3	kilo pascal (kPa)
ktap	1.000 000 X E +2	newton-second/m^2 ($N-s/m^2$)
micron	1.000 000 X E -6	meter (m)
mil	2.540 000 X E -5	meter (m)
mile (international)	1.609 344 X E +3	meter (m)
ounce	2.834 952 X E -2	kilogram (kg)
pound-force (lbs avoirdupois)	4.448 222	newton (N)
pound-force inch	1.129 848 X E -1	newton-meter (N•m)
pound-force/inch	1.751 268 X E +2	newton/meter (N/m)
pound-force/foot^2	4.788 026 X E -2	kilo pascal (kPa)
pound-force/inch^2 (psi)	6.894 757	kilo pascal (kPa)
pound-mass (lbm avoirdupois)	4.535 924 X E -1	kilogram (kg)
pound-mass-foot^2 (moment of inertia)	4.214 011 X E -2	kilogram-meter^2 ($kg•m^2$)
pound-mass/foot^3	1.601 846 X E +1	kilogram/meter^3 (kg/m^3)
rad (radiation dose absorbed)	1.000 000 X E -2	**Gray (Gy)
roentgen	2.579 760 X E -4	coulomb/kilogram (C/kg)
shake	1.000 000 X E -8	second (s)
slug	1.459 390 X E +1	kilogram (kg)
torr (mm Hg, 0° C)	1.333 220 X E -1	kilo pascal (kPa)

*The becquerel (Bq) is the SI unit of radioactivity; 1 B_q = 1 event/s.
**The Gray (Gy) is the SI unit of absorbed radiation.

TABLE OF CONTENTS

LIST OF ILLUSTRATIONS

LIST OF TABLES

SECTION 1

INTRODUCTION

The study of artificially-created plasma clouds in the ionosphere is important because of the effects on propagation that they produce. These effects are produced by the generation of small-scale structures or striations (irregularities in the electron concentration* aligned with the earth's magnetic field). Our understanding of the phenomena that occur and the physical processes that control them has been advanced by a combination of analytical work, numerical simulation, observations made during field experiments, and data analysis and interpretation. This report describes some activities in support of the Defense Nuclear Agency's (DNA's) programs in these areas.

Section 2 describes Science Applications International Corporation's (formerly named Science Applications, Incorporated and hereinafter referred to as SAI) participation in the DNA-sponsored PLACES and Midnight Sky field operations. PLACES (Position Location And Communications Effects Simulations) was a field experiment to demonstrate and investigate the effect of structured ionospheric plasma on satellite communication and navigation systems. The structured plasma environment was created by four releases of barium vapor (on separate evenings) carried by rockets to the 180-185 km altitude regime near Eglin Air Force Base, Florida in December, 1980. The behavior of the resulting ion clouds and the study of the evolution of their striations were secondary objectives of PLACES. These objectives

---

* Electron concentration and total ion concentration are equal to each other and will be used interchangeably throughout this report. Electron density or ion density is used sometimes to denote the same quantity when expressed in units of cm^{-3} or m^{-3}.

were to be met in part by flying rocket-borne transmitters behind (as seen from the ground) and rocket-borne plasma probes through the structured ion cloud. These tasks required that each ion cloud be released in a limited spatial region due to safety and rocket performance limitations, and accurately located in real time so that its position ten or more minutes in the future could be predicted.

In Section 2.1.1 we describe the operational plans and tracking procedures used to accomplish these tasks as well as their limitations. In Section 2.1.2 we report the release points and ion cloud motion as well as various factors that impacted the outcome. We conclude in Section 2.1.3 with a suggestion for making use of the alignment of the ion cloud with the magnetic field as an aid for minimizing the miss distance between the actual and optimal aim points if this real-time capability is desired in the future.

Midnight Sky was a field operation conducted near Fairbanks, Alaska in March and April, 1981. Its primary purpose was to obtain optical data related to striation freezing. Two modest-sized barium releases were deployed in the 190 km altitude range. A major task was to obtain pictures of the ion cloud looking up the magnetic field in order to determine the configuration of striations and their evolution. This task was to be accomplished by flying a small aircraft with a mounted TV and still cameras on a trajectory that would intercept the path of the moving footprint of the ion cloud projected down the magnetic field lines. In Section 2.2 we describe the plan and procedures and their implementation, the results obtained, and recommendations for improvements if such an attempt were to be tried again.

SECTION 2

FIELD TEST PARTICIPATION

This section describes SAI's participation in the DNA-sponsored PLACES and Midnight Sky field operations. The objectives of these programs, some operational requirements that they imposed, plans and procedures developed to satisfy those requirements, some results obtained, and recommendations for carrying out similar operations in the future are discussed.

2.1 PLACES.

PLACES (Position Location And Communications Effects Simulations) was a field experiment to demonstrate and investigate the effect of structured ionospheric plasma on satellite communication and navigation systems. The structured plasma environment was created by four releases of barium vapor (on separate evenings) in the 180-185 km altitude regime in December 1980 near Eglin Air Force Base, Florida. The behavior of the barium ion clouds and the characteristics of the structured ionization were secondary objectives of PLACES. These objectives were to be met in part by flying rocket-borne transmitters behind the structured ion cloud (as seen from the ground) and rocket-borne diagnostic instruments through the structured plasma. Four beacon rockets and two probe rockets were available to be targeted during the events.

Range safety and performance limitations on the beacon and probe rockets restricted the ion cloud location to a limited region at the time of the passage of the beacon and/or probe rocket. The barium release location had to be chosen carefully so that the ion cloud would have time to structure and be in the proper location at the time of the beacon and/or probe rocket

passage. The line-of-sight (LOS) from the beacon rocket through the ion cloud had to pass through the beacon-receiver ground sites. Sufficient time had to be allowed for the ion cloud to separate from the neutral cloud so that the center of the dense portion of the ion cloud could be identified and then tracked. The ion cloud motion had to be determined sufficiently accurately to predict the ion cloud location ~ 10 minutes or more in the future. The corresponding beacon/probe rocket was then targeted and launched, and then it traveled to the desired aim point. By this time (more than ~ 20 minutes after release) the ion cloud was expected to have developed sufficient structure. Past experience with 48 kg barium releases at Eglin AFB has indicated that sufficient structure would develop in approximately 1.5-2 striation onset times.

SRI International (SRI) had primary responsibility for tracking the ion cloud using optical TV trackers at two stations (Ref. 1). Sandia National Laboratories - Albuquerque (SNLA) had primary responsibility to process and use the raw TV-track data, predict the future ion cloud position at the appropriate time, target the desired aim point, determine the rocket launch angles and launch the rockets (Ref. 2). Science Applications, Inc. (SAI) provided guidance in the field for optimizing procedures to be followed in real time and provided quick-look assessments of the behavior of each ion cloud with recommendations for the following event. Close interactions with and cooperation of N. Chang of SRI and L. Rollstin of SNLA are gratefully acknowledged and lead to the successful achievement of the test objectives.

In the following sections we describe the results of carrying out the above tasks and recommendations for future attempts to implement them.

2.1.1 Operational Plans and Tracking Procedure.

Many barium releases conducted in the previous fifteen years at Eglin AFB, particularly Project SECEDE-II in January 1971 and Project STRESS in February 1977, have shown that the neutral wind at 180 km altitude typically blows towards the east at 50-120 m/s at dusk. The dense portion of large ion clouds tends to move in the same general direction but more southerly at half the speed (due to an ambient ionospheric electric field). Indeed, the motion of the dense portion of all large ion clouds during the first 30 minutes following a dusk release at Eglin AFB was towards the east or southeast with a heading that lay within the azimuth limits of 70^{o} to 146^{o} (degrees east of north). Furthermore, by the time such clouds had moved 40 km from their release point, they had developed sufficient structure so as to be useful for the test objectives.

Based on this experience and range safety and rocket performance criteria, a nominal release point of 29.27^{o} N latitude and 87.37^{o} W longitude was chosen for the first event. Figure 1 shows the location of the nominal release point, azimuth limits, the 40 km locus, the launch site at A-15A on Santa Rosa Island, beacon receiver sites at D-3 and on St. George Island, and optical sites located at Tyndall AFB, C-6, and A-105 approximately 3 miles west of the launch site. The FPS-85 radar, operated in an incoherent scatter mode and used for ion cloud tracking and measurement, was located at Site C-6.

The nominal release point was chosen as far west and north as possible and still allow a beacon rocket fired at a maximum azimuth of 210^{o} (due to range safety considerations) to pass sufficiently far to the west on its downleg to obtain a useful occultation of the beacon vehicle by the structured ion cloud as seen by the beacon receiver sites. Release positions further east jeopardized firing a late-time probe rocket at a structured cloud if it moved rapidly to the east. An ion cloud located along the northern azimuth boundary of 70^{o} required a

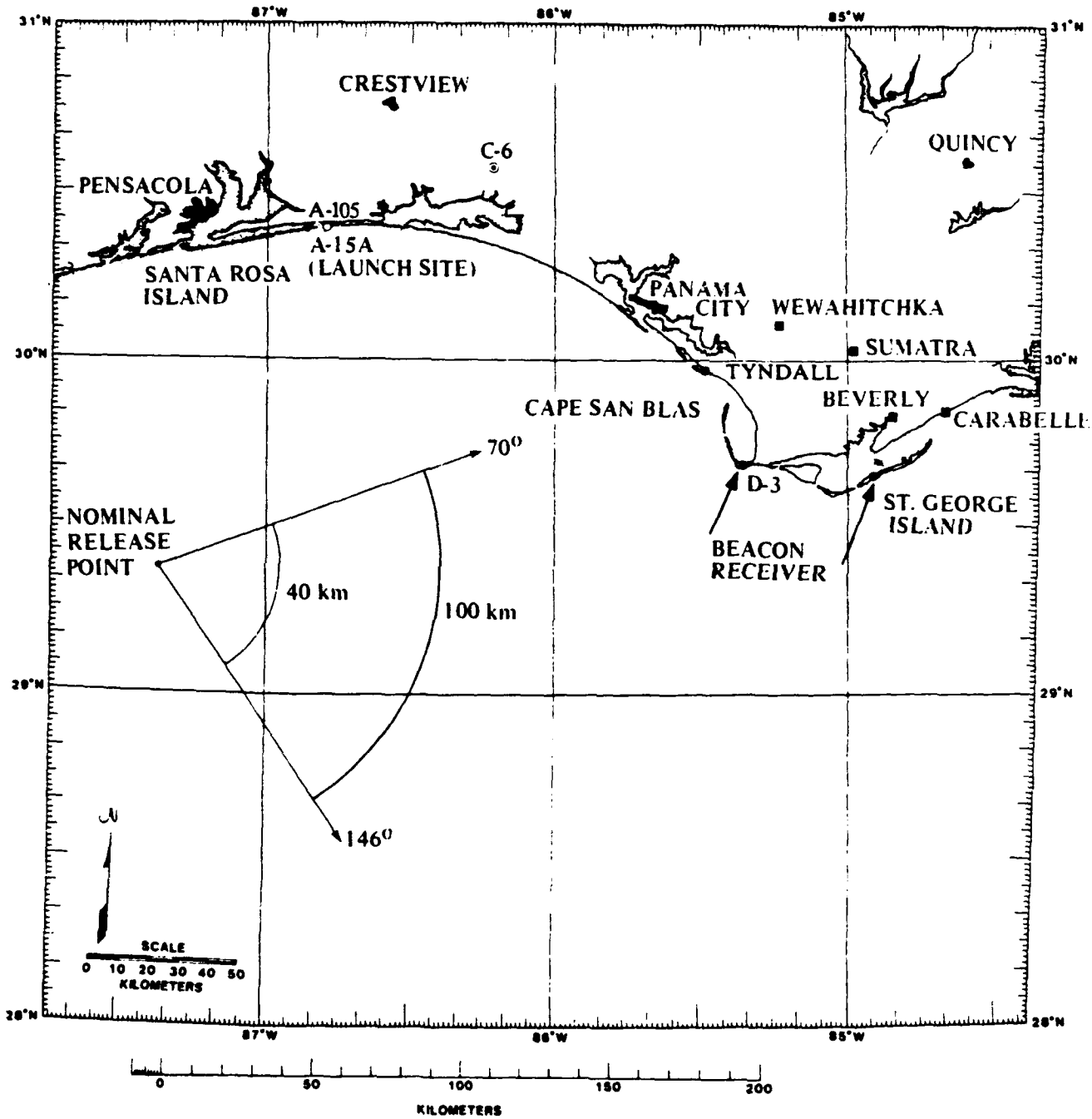

Figure 1. Eglin AFB Gulf Test Range and nominal release point for PLACES events.

nominal elevation-launch angle for the beacon rocket in excess of 85° which was the maximum considered prudent under typical wind conditions.

The four events were named GAIL, HOPE, IRIS, and JAN, an alphabetical continuation of the female names used during the STRESS test series. The tentative plan was to fire a beacon and probe rocket during Events GAIL and IRIS and two beacon rockets in conjunction with Event HOPE. A probe rocket was to be fired after a beacon rocket so as to pass through the structured portion of the ion cloud simultaneously with the beacon occultation. Any unused comparison rockets would be used with Event JAN. The time of the initial release, GAIL, was chosen as 5 minutes prior to a solar depression angle (SDA) of 6° as a trade off between having the cloud still illuminated at a late time and a sufficiently dark sky early in order to produce a good image of the ion cloud for tracking purposes.

The TV-trackers were located at Site D-3 near one of the beacon receivers and about 400 m north of the rocket launch pad at A-15. The TV-trackers were planned to be used during the 30-40 minute duration when the ion cloud was illuminated. The TV-tracker at Site D-3 was designated as prime for the beacon rocket because it had the same view of the ion cloud as did the beacon receiver. The A-15 tracker was designated as prime for the probe rocket because its view of the cloud contained the plane of the probe rocket trajectory. For each rocket, a target point was to be determined by using the prime TV tracker line-of-sight and an altitude determined either by its intersection with the vertical plane determined by the line-of-sight of the other TV-tracker or by an empirical height variation that was consistent with the settling of the ion cloud. Because the quality of data obtained by using a two-station solution has lead to practical difficulties in the past, it was not used for PLACES.

A more detailed discussion of the problems associated with targeting barium ion clouds in real time, as well as sug-

gested improvements, is contained in Section 2.1.3. In the next section we describe the initial release location and motion of each of the ion clouds.

2.1.2 Release Points and Cloud Motion.

Much of the information and discussion presented here has relied heavily on information contained in References 1-5. Table 1 summarizes the release times and coordinates for each of the four events. The release times are taken from Rollstin and Wyatt (Ref. 2) and represent the time of initiation of the thermite reaction. These times are generally within a second or so of times reported by others who observed optical or radar signatures. For each event, three sets of release coordinates are given. In order they are: the planned release coordinates; the radar-determined position of the rocket at the time that the barium thermite release was initiated (Ref. 2); and the optically determined burst point based on images of the neutral cloud in the first seconds after release (Ref. 5). The estimated accuracy of the last two data sets is $\sim 0.004^{o}$ or ~ 0.4 km.

The differences between the planned and actual release-initiation coordinates are discussed thoroughly in Ref. 2. The actual 4-6 km lower altitudes was attributed to slightly slower burning first-stage motors than expected and slightly heavier second stage vehicles than expected. The ten kilometer altitude difference for the Event IRIS was attributed to an abnormal second-stage ignition-time delay. The 4 to 7 km displacements in latitude and longitude are less than the expected dispersion for these rockets.

The optically-determined release locations are all reported as being higher in altitude, further south and further west than the position of the rocket at release ignition. These displacements are all generally in the same direction that the rocket was heading and are due to the vapor cloud traveling with the rocket until it slows down by transferring its momentum to

Table 1. PLACES events release coordinates.

Event	Date (LT)	Time (GMT)	Altitude (km)	Latitude (°N)	Longitude (°W)	Displacement (km)
			185.0	29.37	87.37	
GAIL	4 Dec	2307:35.8	178.8	29.329	87.402	
			181.3	29.317	87.420	3.3
			185	29.25	87.0	
HOPE	6 Dec	2307:37.9	180.9	29.278	87.030	
			182.6	29.263	87.042	2.7
			190	28.833	87.167	
IRIS	8 Dec	2313:07.3	179.6	28.796	87.167	
			182.2	28.763	87.185	4.8
			190	29.167	86.917	
JAN	12 Dec	2313:41.6	182.5	29.188	86.974	
			183.7	29.176	86.978	1.8

the ambient atmosphere. The magnitude of the observed displacements of 2-3 km (except for IRIS) are consistent with this cloud expansion and slowing down description. The apparent larger displacement of IRIS could be the result of its greater range from the optical sites or possibly its determination a few more seconds after burst.

In the next section we summarize the results of tracking the ion clouds in chronological order.

2.1.2.1 Event Gail. The primary tracking mode to target the beacon rocket for this event was to use the intersection of the D-3 beacon TV-tracker look axis with the vertical plane defined by the probe TV-tracker at A-15. Unfortunately, the beacon TV-tracker operator at site D-3 tracked the neutral cloud, which was traveling north northeasterly, well into the event rather than the ion cloud until after the latter had striated. The result was to produce a well-defined track with a larger northward and smaller eastward velocity than the ion cloud actually had. The reportedly large northern velocity placed the predicted location of the ion cloud too far north to allow a beacon rocket to be fired. When the beacon TV-tracker operator began adjusting to the well-striated ion cloud, the apparent track became erratic and it was difficult to make useful predictions of cloud location.

Although it appeared to observers at A-15 that the ion cloud was not so far north and the ion cloud image was well-defined, this error was not discovered in real time. Indeed, the apparent position of the ion cloud stopped its northward motion around R + 26 min (R refers to the release time) and never reached an elevation exceeding 62° as seen from A-15. Table 2 lists the estimated initial velocities of the four ion clouds. Figure 2 shows the optically determined release locations and arrows showing the direction of the initial motion of each cloud. The length of the arrow is proportional to the speed and the tip represents the location of the ion cloud after 25 minutes. The

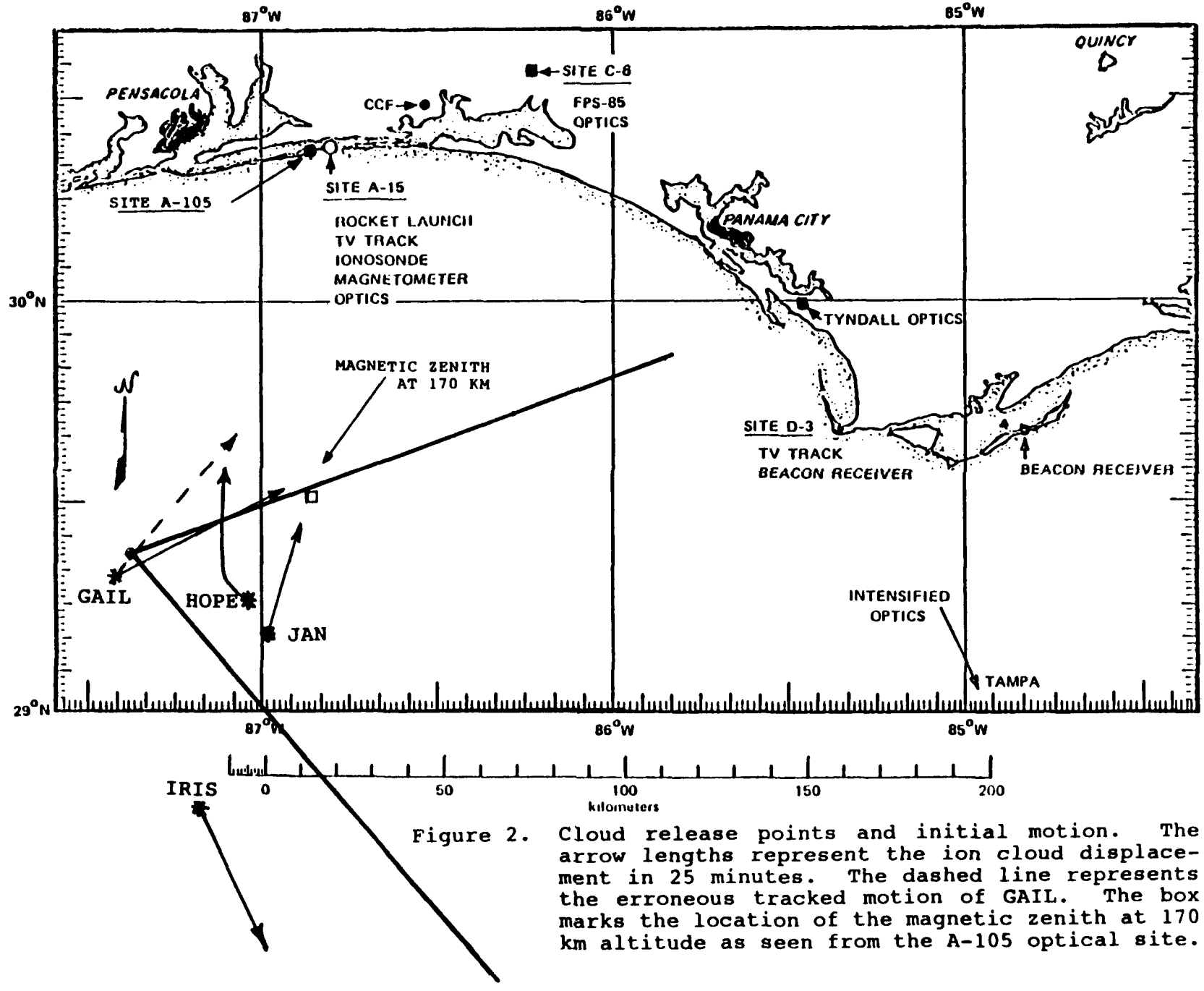

Figure 2. Cloud release points and initial motion. The arrow lengths represent the ion cloud displacement in 25 minutes. The dashed line represents the erroneous tracked motion of GAIL. The box marks the location of the magnetic zenith at 170 km altitude as seen from the A-105 optical site.

TABLE 2. Initial ion cloud motion and distance traveled in 20 minutes.

Event	East (m/s)	North (m/s)	Speed (m/s)	Direction (Azimuth)	Distance (km)
GAIL	34 ± 2	18 ± 3	39 ± 2	62° ± 4°	17
HOPE					
(<R+15)	-15	15 ± 2	21 ± 2	315°	24
(>R+20)	~2			6°	
IRIS					
(<R+15)	20	-28	34	144°	29
(>R+17)	26	-17	31	123°	
JAN	9	26	28	19°	33

dashed arrow for GAIL represents the erroneous ion cloud track reported to be moving at 57 m/s at an azimuth of 29°.

Also shown in Figure 2 is the original nominal release point and the operational azimuth limits defining the area where the ion cloud must be in order to obtain a beacon occultation with the beacon passing 100 km behind the ion cloud. It can be seen that even if an accurate ion cloud track had been obtained, a beacon rocket launch would still have been prevented due to the northerly motion of the ion cloud. A probe rocket would not have been prevented by range safety considerations had an accurate track of the ion cloud been available. However, there was no plan to launch a probe rocket without a previous beacon rocket.

Figure 2 also shows a small square located at the magnetic zenith at an altitude of 170 km as seen from the launch pad at Site A-15. The magnetic zenith is defined as that point in the sky such that the line-of-sight from the observer is tangent to the magnetic field at the specified altitude. The striations of an ion cloud located at the magnetic zenith are

parallel to the line-of-sight so that the configuration of the ion cloud perpendicular to the magnetic field can be seen. It is apparent that GAIL moved towards the magnetic zenith as seen from A-15. This fortuitous circumstance greatly foreshortens the extended length of the ion cloud parallel to the magnetic field and presents a rather well-defined target for aiming the probe TV-tracker.

Because it is very difficult to determine the altitude or distance along the look-line to the center of the cloud, and without vertical winds ion clouds gradually settle under the influence of gravity, it was decided to use an empirical height relationship (derived from a fit to the STRESS Event ANNE) in conjunction with the probe TV tracker for the next event. This decision was further enhanced by the fact that the D-3 operator had no ion filter and thus had to track the neutral cloud for the first 5-10 minutes until the ion cloud was well separated and identifiable on the TV-monitor.

2.1.2.2 Event HOPE. It was decided to move the release point for Event HOPE to the east and southward (as shown in Table 1) to allow for more northerly motion. It was also decided that a probe-rocket launch could be allowed in the event that the beacon rocket could not be launched. A slow scan image was sent from D-3 to A-15 along with the aiming point so that an indication of the quality of the two-station solution could be made. However, because of the delay in receiving a full picture, there were limitations to its real-time usefulness.

Event HOPE did not move in a straight path during the initial 35-40 minute duration of optical tracking. It initially moved northwest at ~21 m/s for the first 12-15 minutes after release, and then moved northerly with a slight eastern drift. As can be seen in Figure 2, the ion cloud was too far north to permit a beacon rocket launch. By the time that a steady optical path was determined (~R + 27 min) the ion cloud was in a location that prohibited a probe rocket launch due to safety reasons.

2.1.2.3 Event IRIS. Because beacon occultations were the highest priority, it was decided to use two beacon rockets and to allow the option of a pass distance of only 40 km behind the cloud, rather than the more optimum 100 km pass distance. This choice allowed a nominal release point slightly west of the HOPE release point. Because of the northerly motion of the previous two ion clouds, and because no probe rockets were planned (probe rockets could not be targeted through the ion cloud if it were too far south), the nominal release point was moved about 0.5 degrees latitude to the south. In order to aid the optical acquisition of the ion cloud, the release time was delayed five minutes (to 6^{o} SDA) so the sky would be darker. It was decided to raise the nominal release altitude to 190 km because: a) the ion cloud Pedersen conductivity would be reduced and the ion cloud would develop striations more rapidly; and b) the ion cloud would be slightly larger presenting a larger target. (The penalty for the larger target size was that the peak electron density would be somewhat reduced.)

As mentioned before, an abnormal tomahawk ignition sequence resulted in a ~10 km lower altitude release than planned. The ion cloud moved southeasterly as indicated in Table 2 and Figure 2. Between 15 and 20 minutes after release, the velocity of the ion cloud moved more easterly as indicated in Table 2. It soon was so far south that the 40 km offset option was chosen. The beacon TV tracker with probe-plane intersection was used to launch the first beacon rocket at R + 25:30 min. The probe TV tracker with empirical height was used to launch the second beacon rocket at R + 38:29 min. The method chosen to determine the aim point was the one that produced a predicted cloud-position that gave a better extrapolation of the real-time track than that of other solutions.

There was considerable scatter in the predicted cloud position due to the method being used. We will discuss the cause of some of this scatter and discuss some ways to deal with it in Section 2.1.3. In part, the scatter results from independent

discrete adjustments in azimuth and elevation as each TV tracker operator attempts to identify a better aim point on the optical image. A second contributing factor was that only a small fraction of the tracking data was available in real time due to limitations imposed by the computer time-sharing network.

The successful occultation with the second beacon was fortuitous. Water clouds began to enter the field-of-view (FOV) at A-15 at about R + 15 min and viewing of the ion cloud between R + 15 min and R + 30 min was sporadic although periodically the striated portion of the ion cloud was easily identifiable. By R + 30 min, Site A-15 was completely covered by clouds and the ion cloud was not seen again. This fact was not communicated to SNLA who continued to use the A-15 tracker to aim the second beacon rocket. The success of this second launch was due to the fact that the TV-tracker operator at A-15 periodically adjusted azimuth and elevation as he had been doing, thus presenting a moderately smooth track although it was not based on any data.

2.1.2.4 Event JAN. A beacon and a probe rocket were planned for Event JAN. This plan plus the southerly motion of the IRIS ion cloud required moving the release point north of that of Event IRIS. Because northern or western motion would limit a planned beacon pass, a nominal release point 5' south and to the east of that of Event HOPE was chosen as indicated in Table 1. As shown in Figure 2, the ion cloud headed towards the magnetic zenith as seen from A-15.

A beacon rocket with a 100-km offset was precluded due to heavy shipping traffic in the predicted impact zone. Difficulty with the field computer for determining nominal launch angles precluded targeting a beacon rocket with a 40-km offset until R + 48 min at which time the ion cloud was too far north. However, the probe rocket was targeted (using the probe TV-tracker and empirical height) with the aid of parametric targeting hand plots that had been prepared prior to the test series. The probe rocket successfully penetrated a high density region of

the JAN ion cloud, reaching a peak density at 110.6 s after launch at R + 31 min.

2.1.3 Real-Time Tracking.

There are a number of difficulties encountered when attempting to track optically a large evolving ion cloud and predict its future location so that a rocket launch may be targeted. One set of difficulties is associated with trying to identify a point in 3-dimensional space that represents a desired feature for targeting. A second set arises when attempting to determine the motion of the desired feature as a function of time (tracking). A third set of problems, which are not addressed here, is associated with targeting a rocket.

The difficulties arise because the ion cloud being tracked is large, diffuse, asymmetric, optically thick in some parts which can hide different features when viewed from different views, and may be partially obscured by the neutral cloud. Furthermore, the ion cloud's brightness is low requiring image intensification by a TV system which forms a higher-contrast image, further obscuring features. These factors cause the image of the cloud to look considerably different when viewed from widely-separated sites. Because the image is large and evolving, it is difficult to identify a single position to track continuously.

A simplified description of the gross distribution of ionization is given here for a cloud ~30 minutes after release. Discussions of the morphology of the development of large barium ion clouds released at 175 - 200 km altitudes are given in References 6 and 7. By ~30 minutes, the ionization has diffused parallel to the magnetic field **B** and is stretched out in a slab-like volume whose typical dimensions perpendicular to **B** may be contained in a rectangular area 4 - 8 km in width and 20 - 40 km in length. The distribution of ionization parallel to **B** is discussed in detail in Reference 8. A typical dimension for the

bulk of the ionization parallel to **B** (e^{-1} point) is 45 km although lower density ionization can be seen optically for 60-70 km along the magnetic field. At these times, the maximum field-line content of an ion cloud produced from a 48-kg barium release at these altitudes is ~2.5 x 10^{17} m^{-2} (Ref. 8). These numbers suggest an average concentration of ~5.6 x 10^{12} m^{-3}, approximately 70% of the expected peak concentration of ~8 x 10^{12} m, for the field lines containing the maximum content.

The configuration of ionization is highly nonuniform in the plane perpendicular to **B**. If the average field line content is half of the maximum value, or 1.25 x 10^{17} m^{-2}, then the field lines containing a total of 6.5 x 10^{24} ions would occupy an area of 52 km^2 or approximately 1/3 of the earlier-mentioned rectangular area. The remaining area contains either lower-density barium ionization or background ionospheric ionization. The highest-density portions of the ion cloud containing striated structure are located nearest to the neutral cloud.

The cross sectional area of interest for tracking is located in a region a few kilometers across perpendicular to **B** and extends tens of kilometers parallel to **B**. Each optical tracker generally picks a point near the "center" of the optical image that contains the apparent highest density striations. Since each site sees a different image of the extended object, it is highly unlikely that they aim at the same spot, or that their respective lines-of-site (LOS) intersect. Several schemes to identify a single point in the ion cloud were developed for tracking purposes and a different scheme using the optical trackers alone, suggested in the field but difficult to implement without having planned for it, is discussed here.

In accordance with Ref. 2, we refer to the optical site at D-3 as the beacon TV-tracker (BTT) and the optical site at A-15A as the probe TV-tracker (PTT). For beacon targeting, two methods to determine a target point were to select the point along the BTT LOS that a) intersected the vertical plane contain-

ing the PTT LOS, referred to here as BTT-P, or b) that intersected a plane at an empirically-determined altitude, referred to here as BTT-H. Likewise, for probe targeting, the equivalent targeting methods are referred to here as PTT-B and PTT-H, respectively.

In order to illustrate the results of applying these techniques, the ion cloud is modeled as a prolate ellipsoid whose center is at 170 km altitude and whose major axis extends 50-60 km parallel to **B** and whose semiminor axes are 4 km. The magnetic field is taken to have a dip of 60^{o} and a declination of 0^{o} for simplicity. A targeting point within an ellipsoid centered on the idealized cloud whose semimajor and semiminor axes are 5.8 km and 1 km, respectively, is considered excellent because it is very difficult to do better and any point within this volume is an equally valid sample. Targeting on a point in an ellipsoid that is twice as large (eight times the volume) is considered acceptable because a cut across the magnetic field lines will reveal the structure and come within 30% of the actual peak <u>in situ</u> or integrated values.

In order to simplify the trigonometry, we use a flat earth coordinate system whose origin is at the center of the ion cloud and whose x, y, and z coordinates point to the east, north, and vertically upwards, respectively. We locate the BTT and PTT optical sites to the east and north, respectively, of the ion cloud such that the elevation angles from each site to an acceptable point on the major axis of the idealized cloud is each 45^{o}. For illustrative purposes we assume that the PTT selects a point on the major axis 10 km in altitude lower than the center while the BTT selects an acceptable point on the major axis at an altitude 10 km above the center. With these choices, the BTT and PTT are located at (180, -5.8, -170) and (0, 165.8, -170), respectively, expressed in kilometers, and the direction cosines of the respective lines-of-sight are (-0.707, 0, 0.707) and (0, -0.707, 0.707).

2.1.3.1 Smallest Sphere of Common Tangency (SSCT). The center of the SSCT is often chosen as the location of a small object determined by triangulation using the nonintersecting LOSs from two fixed sites of known separation. This method is not appropriate for extended barium ion clouds. The direction cosines of the diameter of the SSCT which connects the points of tangency is given by the cross product of the direction cosines of the BTT and PTT LOSs or (0.577, 0.577, 0.577), i.e., it points upwards from the PTT LOS and to the northeast. If $\mathbf{L_p}$ and $\mathbf{L_b}$ are the vectors from the intersection of the PTT LOS and BTT LOS with the axis of the ion cloud to their respective intersections with the vector **D** representing the diameter of the SSCT from the PTT LOS to the BTT LOS, then $\mathbf{L_p} + \mathbf{D} - \mathbf{L_b} = \mathbf{L}$ where $\mathbf{L} = (0, -11.55, 20)$ is the vector expressed in kilometers along the magnetic field from the intersection of the PTT LOS with the cloud axis to the intersection of the BTT LOS with the cloud axis. By writing the magnitudes of these four vectors as L_p, D, L_b, and L, respectively, we obtain three equations for L_p, D, and L_b in terms of L = 23.1 km:

$$
\begin{aligned}
0 \quad &+ \quad 0.577\,D \quad - \quad 0.707\,L_b \quad = \quad 0 \ ; \\
-0.707\,L_p \quad &+ \quad 0.577\,D \quad + \quad 0 \quad = \quad -11.55 \ ; \\
0.707\,L_p \quad &+ \quad 0.577\,D \quad + \quad 0.707\,L_b \quad = \quad 20 \ .
\end{aligned}
$$

The solution gives D = 4.9, L_p = 20.3, and L_b = 4.0 in km. The center of the SSCT is located at $\mathbf{L_p} + \mathbf{D}/2$ from the intersection of the PTT LOS with the axis of the cloud at 160 km altitude. In the coordinate system centered on the ion cloud center, the center of the SSCT is located at (1.4, -7.2, 5.8), a distance 9.4 km from the center of the ion cloud and 3.6 km from the field line on which the ion cloud is located. This procedure is unacceptable for determining a tracking point in the ion cloud.

2.1.3.2. BTT-P, BTT-H, PTT-B, and PTT-H. Table 3 summarizes the results of using either the intersection of the BTT or PTT LOSs with either the vertical plane defined by the other LOS or a constant altitude plane here taken to be the

Table 3. Triangulation method results.

Method	Target Coordinates (km)	Distance from B (km)	Distance along B (km)	Quality
SSCT	(1.4, -7.2, 5.8)	3.6	8.6	Unacceptable
BTT-P	(0, -5.8, 10)	0	11.6	Acceptable
BTT-H	(10, -5.8, 0)	11.2	2.9	Unacceptable
PTT-B	(0, -5.8, 1.6)	4.2	4.3	Unacceptable
PTT-H	(0, -4.2, 0)	3.6	2.1	Unacceptable
Field Line	(0, 0, 0)	0	0	Excellent

altitude of the center of the ion cloud at 170 km. All coordinates are given in kilometers with respect to the center of the ion cloud. Of these four methods, only one, BTT-P, produced an acceptable result in terms of locating a point that was near the magnetic field line containing the maximum concentration. The only reason that the BTT-P method was acceptable in this simplified geometry was because the field-aligned axis of the cloud lay in the vertical plane defined by the PTT LOS. If this condition had not been chosen, the PTT-B would also have produced an unacceptable result.

The two points determined using the BTT LOS would have been acceptable for determining a target point for launching a beacon rocket because the LOS to the beacon rocket would have cut through the ion cloud near enough to its center. Likewise, as long as a probe rockets' trajectory passed through the target point at an angle greater than 24^{o} with respect to **B**, it too would cut through the acceptable (high density) portions of the cloud. However, a rocket trajectory passing through the PTT-B determined point at an angle less than 16^{o} with respect to **B** would miss the high density portions of the ion cloud.

One problem with these four methods for predicting the motion of ion clouds is the variability that they introduce in the triangulation points when equally-acceptable points on the image of the ion cloud are identified by the two TV-trackers. For instance, if the points identified by the two TV-trackers were reversed, the resulting target coordinates would be approximately reflected about the origin (or cloud center). These coordinates would represent a shift of 8 km to 23 km in target aim point. Apparent shifts in cloud position of these magnitudes, not associated with motion of the cloud, make accurate tracking for prediction purposes difficult.

2.1.3.3. Field Line Motion. The most accurate way to locate an ionospheric ion cloud is to identify the field line that passes through the point of interest and then specify its approximate altitude. The problem with the above methods of attempting to locate the cloud is that necessarily large errors in identifying the altitude of the cloud were translated into unnecessarily large errors in identifying the field line on which the cloud is located. For tracking purposes, the altitude of the maximum density in the cloud need not be known to within ± 10 km if the field line through the point of interest is known to within ± 2 km. If the two LOSs are projected into the plane perpendicular to $\mathbf{B}$, their intersection determines the field line. The altitude can be determined either by averaging the altitudes of the intersection of each LOS with the field line, or by using an approximate altitude. The last entry in Table 3 shows that this method applied to the hypothetical situation discussed above produces an excellent result. Furthermore, interchanging the aim points of the two LOSs produces no shift in the target coordinates.

The method of locating the field line needs to be modified when the ion cloud approaches the magnetic zenith of one of the sites, taken here to be the probe site. The magnetic zenith is that LOS which is tangent to the earth's magnetic field

at the altitude of the maximum density of the ion cloud. In the flat earth system, it is the field line passing through the site. As an example, the LOS to an ion cloud less than 20 km from the magnetic zenith at an altitude 170 km makes an angle of $< 7^{o}$ with **B**. A 2-km error in locating the desired field line will result in a greater-than-14-km misidentification of the correct altitude. A better method of locating the desired field line is to use a one station solution by identifying an appropriate altitude along the desired LOS. A 10-km uncertainty in the correct altitude, on the other hand, misidentifies the correct field line by only 1.5 km. An approximate altitude can be used (discussed below) or the altitude of the point of closest approach of the other LOS.

When the ion cloud is located at the magnetic zenith, the desired field line can be selected with no error. It is much more difficult to identify the altitude of the peak density accurately but it need only be found to within ± 10 km to be acceptable. An estimate of the altitude of the ion cloud can be made based on the analysis given in Ref. 8 which is summarized below.

Because the barium ion is much heavier than atmospheric neutrals, gravity places a body force on the ion cloud equivalent to a neutral wind $\mathbf{g}\,\tau$ where $\mathbf{g}$ is the effective acceleration due to gravity (accounting for the bouyancy of the displaced air molecules) and τ is the effective barium-neutral collision time for momentum exchange. Thus the effective neutral wind velocity acting on the ion cloud is

$$\mathbf{U} = \mathbf{V}_a + \mathbf{g}\,\tau \qquad (1)$$

where $\mathbf{V}_a$ is the ambient neutral wind at the center of the cloud. A low-density plasma moves with $\mathbf{E} \times \mathbf{B}/B^2$ in the large $\Omega\tau$ limit where $\Omega = eB/M$ is the ion gyrofrequency and $\mathbf{E}$ is the frame-dependent electric field. Large-conductivity barium clouds partially polarize and acquire only a fraction of the velocity

resulting from the electric field, E_o, seen in the frame moving with velocity U, or

$$E_o = E_a + U \times B \qquad (2)$$

where E_a is the ambient electric field. The ion cloud center thus moves approximately as

$$V_c = U + (1-\eta)\, E_o \times B/B^2$$

$$= U_{\parallel} + \eta\, U_{\perp} + (1-\eta)\, E_a \times B/B^2 \qquad (3)$$

where $U_{\parallel}$ and $U_{\perp}$ are the components of U parallel and perpendicular to B, respectively, and $\eta(\alpha)$ is a function of $\alpha = \Sigma_p^c/\Sigma_p^a$ which is the ratio of the enhanced field-line-integrated Pedersen conductivity due to the cloud to that of the ambient ionosphere. The coupling parameter $\eta(\alpha)$ which measures the fraction of the effective neutral wind that the ion cloud moves with increases monotonically from 0 to 1 as α increases from 0 to ∞. For a cylindrically symmetric model ion cloud with uniform density inside a finite radius and ambient density outside, $\eta(\alpha) = \alpha/(2+\alpha)$, (Ref. 9). Clouds with more realistic density profiles are slightly less coupled (Refs. 10 and 11). The observed value of η for the first three PLACES clouds was 0.67 ± 0.03 while Jan was less coupled to the neutrals with $\eta \sim 0.52 \pm 0.03$.

The velocity $U_{\perp}$ in Eq. (3) is given by Eq. (1) strictly only for α very large or for V_a independent of altitude. Careful analysis (Ref. 8) shows that there is a conductivity-ratio-dependent term that modifies $U_{\perp}$ if the ambient Pedersen-conductivity-weighted field-line-integrated neutral wind perpendicular to B differs from $V_{a\perp}$ at the cloud center. We ignore this difference here.

For illustration, we consider a northward magnetic field (0^o declination) with dip angle θ, a neutral wind with northward and downward components V_N and V_D, respectively, and

the westward component of the ambient electric field, E_w. (Eastward neutral winds and northward electric fields do not produce vertical motion of ion clouds.) The downward speed of the ion cloud is then given by

$$V_{cD} = V_D + g\tau + (1-\eta)\cos\theta \{E_w/B + V_N \sin\delta - (V_N + g\tau)\cos\theta\} \quad (4)$$

where $g = |g|$. With $\theta = 60^o$ and $\eta = 0.6$, Eq. (4) becomes

$$V_{cD} \sim 0.9(V_D + g\tau) + 0.2(E_w/B + 0.9V_N). \quad (5)$$

The electric field is independent of altitude and $g\tau$ varies inversely with neutral density. The northward and vertical motions of the neutral wind may have both variations with altitude due to tidal motions, acoustic gravity waves, or disturbed air flows.

We may obtain an explicit expression for the altitude $h = h(t)$ of the center of the ion cloud as a function of time by assuming that the atmospheric density profile is exponential with a neutral atmospheric density scale height H_n. With this assumption, the form of the downward speed of the ion cloud is

$$V_{cD} = V_1 + V_2 \exp[(h - h_o)/H_n] = dh/dt \quad (6)$$

where h_o is the initial altitude. V_1 and V_2 can be obtained from Eq. (4) or (5) when both V_D and V_N are assumed to have the same as in Eq. (6). This equation may be integrated to give the explicit time-dependence of the change in altitude of the peak concentration of the ion cloud as

$$\Delta h = h(t) - h_o = -H_n \ln[(1 + V_2/V_1)\exp(V_1 t/H_n) - V_2/V_1]. \quad (7)$$

If the downward velocity varies inversely with the neutral density, $V_1 = 0$, then

$$\Delta h(t) = - H_n \ln(1 + V_2 t/H_n). \quad (8)$$

V_2 can represent g_T plus a flux-conserving downward neutral density flow.

Example calculations of the downward motion of ion clouds as well as the change in density profile parallel to **B** are given in Ref. 8. The values H_n = 22 km and V_2 = 12 m/s were found to be reasonable numbers that matched the descent of the Spruce ion cloud in Secede II and the Ann ion cloud during the STRESS test series. These values were used in Eq. (8) during PLACES to provide an estimate of the height of the ion cloud for use with a single-station LOS (Ref. 2).

2.1.3.4 Real-Time Tracking. A single-station operator does not provide a continuously-varying LOS for several reasons. One reason is that the cloud image presents a large target area in which the optimal point is uncertain. After a short time, even though the ion cloud may have moved and changed shape slightly, the LOS may still represent an equally-acceptable aim point. The operator is not likely to change his LOS until the cloud has moved sufficiently, perhaps several kilometers, to make it apparent that there is a better aim point. A cloud moving 17 to 34 m/s takes a minute or two to move 2 km. When a new aim point is selected, it is very likely to be at a different altitude even if it passes close to the same field line.

Uncorrelated changes in aim point from two sites leads to large random variations in the apparent motion of the cloud which ordinarily moves in a smooth track. A tracking scheme which weights these changes will have a wide scatter in projected future positions. In post-event analysis, a sequence of photographs taken at nearly the same times (usually within $\pm$ 15 s) from two or more sites are used. One technique that is particularly helpful is to project the LOS from the complementary site into each site's field-of-view (FOV) with altitude markers on the projected LOSs. These LOSs can be used to guide adjusted LOSs in each FOV to reduce the miss distance sufficiently so that

the uncertainty in the location of the field line that is identified is <0.4 km.

In real time, this projection has not been used. The center of the SSCT has been projected onto the TV FOV but, as shown earlier, this position does not correlate well with the field line trying to be identified due to differences in appearance and variation in altitude. Furthermore, iteration is very difficult unless the same observer sees both views. An observer with only one view is likely to be influenced, positively or negatively, by the observed discrepancy - they both could iterate to an undesirable point but feel "justified" because they both are on it.

An optimal technique yet to be developed would be to identify a common field line with an iteration scheme that would reach an agreed to altitude. Until that technique is developed, each site should make an independent assessment of its best aim position at set time intervals at least a minute apart at midlatitudes (1 1/2 to 2 minutes is probably optimum). For each new measurement, each site should disregard its previous aim point, examine the image to select the next aim point, and aim the pointer so that the coordinates of the LOS will be ready to read at the next agreed time marker. These coordinates should not be read or recorded until the operator has indicated that his aim is set. Coordinates at each site should be recorded simultaneously. Coordinate values between set times should not be used. The time intervals between measurements can be used to adjust filters, diaphragms, magnification, etc, and other housekeeping chores.

The track of the field line with a smoothly-varying altitude should eliminate large random jumps in the apparent location of the cloud. Of course, if the operator realizes that he has been tracking in incorrect feature, those data points should be ignored and greater weight placed on aim points of

which he is certain. Past experience has indicated that the direction and speed of the intersection of the triangulated field lines with a constant altitude plane can be determined to an accuracy of $\pm 3^{o}$ and $\pm 5\%$, respectively. Thus the position of an ion cloud traveling at 40 m/s can be projected 10 minutes into the future with a ± 1.2 km uncertainty in its expected position.

2.2 MIDNIGHT SKY.

Midnight Sky was a field operation conducted near Fairbanks, Alaska in March and April, 1981. Its primary purpose was to obtain optical data related to striation freezing Two modest-sized barium releases were deployed in the 190 km altitude range. A major task was to obtain pictures of the ion cloud looking up the magnetic field in order to determine the configuration of striations and their evolution. This task was accomplished by flying a small aircraft with a mounted TV and still cameras on a trajectory that would intercept the path of the moving footprint of the ion cloud projected down the magnetic field lines.

The logistics of organizing the Midnight Sky field test and arranging for the small aircraft were carried out by Herb Mitchell, then at R&D Associates, Arlington, Virginia. Eugene Wescott and Tom Hallinan and staff at the University of Alaska provided ground optics and T.V. coverage that could be used for cloud tracking purposes. W. P. Boquist of Technology International Corporation provided ground optics and T. V. coverage of cloud phenomenology. The Chatanika radar was used to monitor the ionospheric electric field for appropriate release conditions. Los Alamos National Laboratories fielded image-intensified optics.

The role of Science Applications, Inc., was to support the overall mission and aid in locating the aircraft at the foot of the field line. In the sections below we describe the payload

and release characteristics, the operational procedures for locating the aircraft, the results obtained, and recommendations for improvements if such an attempt were to be tried again.

2.2.1 Payload and Release Characteristics.

A new chemical formulation was used in Midnight Sky. The standard chemistry involved the oxidation of barium by cuprous oxide to produce heat to liquify and vaporize excess barium according to the formula

$$CuO + 2.5\ Ba \rightarrow Cu + BaO + 1.5\ Ba.$$

Past experience has shown that in this altitude range from 5% to 10% of the chemical payload weight ends up as barium vapor that can be ionized by sunlight.

The new chemistry used in canisters A and B for Midnight Sky was based on the reaction of titanium with boron to produce heat to vaporize barium according to the formula

$$Ti + 2B + xBa(s) \rightarrow TiB_2 + xBa(g).$$

It is claimed that this formulation is four times more efficient (Ref. 12) at producing atoms of barium vapor than the standard chemistry which was used for Spruce during Secede II, but no field test data have been presented to substantiate this claim. It is also claimed that this new release formulation produces "prompt" ionization in times short compared to photoionization times.

Properties of the payload characteristics of canisters A and B and one of the three 16 kilogram canisters used for Spruce are summarized in Table 4. The first four items for canisters A and B are taken from reference 12. Theoretically, the maximum value of x in the above equation is 0.66 (Ref. 13)

Table 4. Payload characteristics.

Canister	A	B	1/3 Spruce
Chemical Wt. (kg)	3.840	4.157	16
Ba Wt. (kg)	1.230	1.386	7.8
% Available Ba	32%	33.3%	48.7%
Ba(g) Atoms	5.1×10^{24}	5.7×10^{24}	5×10^{24}
Altitude (km)	199	199	200
Model Σ_p^c (mho)	-	-	12
Time of formation	<< 10 s		~12 s

resulting in an approximately 56% efficient chemical mixture by weight. The actual canisters used contained approximately 33% Ba corresponding to x ~ 0.17. The fourth line represents the claimed factor of four *increase of efficiency*. Model calculations (Ref. 14) of the expected field-line-integrated Pedersen conductivity of the cloud, Σ_p^c, result in a value of 12 mho at the 200 km altitude of these releases. The number of ions produced by the two Midnight Sky releases are discussed Section 2.2.3. Ions were observed to be formed rapidly in the first ion cloud, in fact, in times short compared to the ion cloud formation time of Spruce.

Two barium releases, named Klondike Kate (KK) and Lady Lou (LL), were conducted during Midnight Sky. The basic characteristics of these two Midnight Sky releases are presented in Table 5. KK moved rapidly to the east in response to large electric fields. The observation window ended for KK due to the bright eastern sky at low elevation. The observation window for LL, which remained rather motionless, ended when the sun set on the cloud. The coupling parameter, η, introduced in Section 2.1.3, and the Pedersen conductivity ratio are discussed in Section 2.2.3 below. Based on the inferred values of the latter,

it is inferred that LL deposited five times as many ions on magnetic field lines as did KK.

Table 5. Release characteristics.

Event	Klondike Kate	Lady Lou
Canister Weight (kg)	~4	~4
Date (local time)	3/29/81	4/2/81
Release Time	19:57	20:25
SDA*	9 1/4°	10°
Altitude (km)	199	199
Motion (m/s)	~450	~±15
Observation Time	~20 Min.	~1 Hour
Measured η	0.18 ± 0.05	0.45 ± 0.05
Inferred Σ_p^c / Σ_p^a	~0.6	~3

*Solar Depression Angle

2.2.2 Operational Procedures.

The ion clouds were expected to move easterly with a speed in the range of 40 to 200 m/s. Our objective was to position the aircraft (a Cessna 402) on the same magnetic field lines as the ion cloud after it had sufficient time (or, equivalently, moved a sufficient distance) for striations to form. A TV camera was mounted in the plane's cockpit pointed vertically to view the ion cloud.

It was necessary to obtain information about the location of both the ion cloud and the plane in real time. The TV tracker at Fort Yukon was used to obtain the azimuth and eleva-

tion of the ion cloud by an experienced observer (Tom Hallinan). The Fort Yukon radar was used to provide range and magnetic heading information. Grids had been prepared with these two sets of information so that both cloud and plane location could be plotted during the flight. The position of the ion cloud was based on an assumed altitude of the nominal 180 km planned release altitude. The origin of the ion cloud grid was displaced 39 km to the north northeast (31° Az.) to account for the inclination (~78°) and declination of the earth's magnetic field near Fort Yukon.

The positioning of the aircraft was based in part on plotting this information and, in part, on the visual appearance of the image of the ion cloud on a small TV monitor in the airplane. Prior to release, the airplane was positioned 40 - 50 km to the magnetic east and several kilometers north of the planned release position heading magnetic south so as to intercept the expected track of the ion cloud.

KK headed to the east at ~450 m/s and the plane could do no more than head east at its maximum speed of ~200 mph or 90 m/s.

LL drifted back and forth causing changes in the initial headings of the aircraft. Figure 3 shows a plot of the positions of the aircraft and the projected footprint of the ion cloud that were traced from the positions recorded in real time. The dashed curve is the projection of the Lady Lou ion cloud path down the magnetic field to the ground, while the solid curve is the track of the instrumented aircraft. The numbers next to the tic marks on the tracks represent the times after release in minutes. The arrow represents the viewing direction from Manley Hot Springs.

During the time period from R + 20 to R + 45 minutes the aircraft was within 20 km of the ion cloud magnetic field line. At R + 28 min, the plane was located on the magnetic field

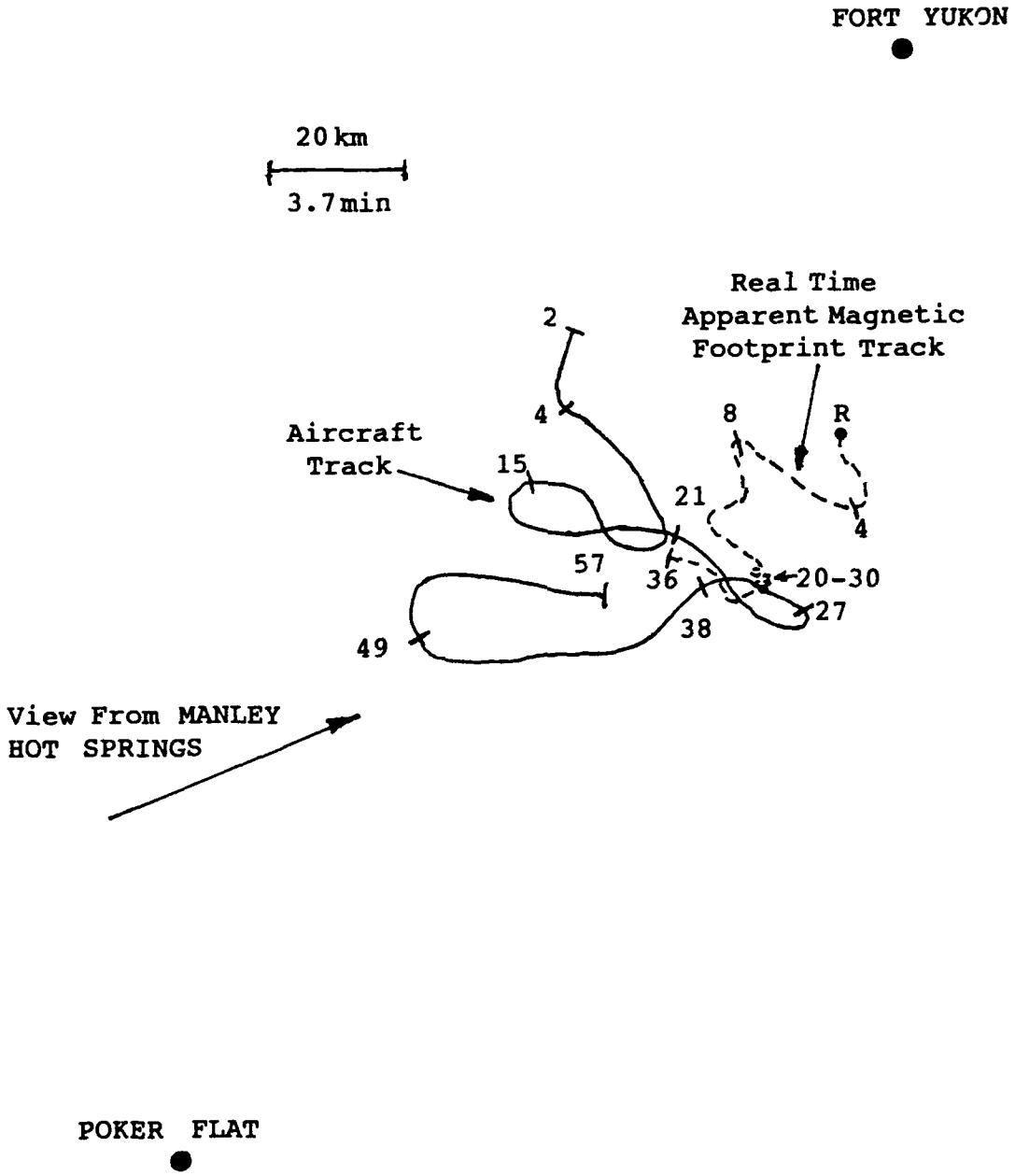

Figure 3. Aircraft and ion cloud tracks during Lady Lou. Numbers by tick marks are minutes after release.

line containing the ion cloud as was confirmed by photographs taken at that time.

2.2.3 Results and Recommendations.

Small and large barium ion clouds, in the sense of the change of the conductivity they induce in the ionosphere, have qualitatively different appearances as sketched in Figure 4. As discussed in Section 2.1.3, small ion clouds have a coupling parameter $\eta \sim 0$ so their velocity is essentially $(\mathbf{E} \times \mathbf{B})/B^2$. In large clouds, most of the ions have a velocity (relative to the neutral cloud) that is smaller than $(\mathbf{E} \times \mathbf{B})/B^2$ by the factor $\zeta = 1 - \eta$, which has a typical value of 0.2 to 0.5. However, some portions of the ion cloud have velocities approaching that of a small cloud, so the large ion cloud becomes stretched out, as indicated on the figure. In addition, for both large and small releases, a bridge of low-level ionization extends between the neutral and ion clouds due to the ions formed at late times by the slow photodissociation of BaO and subsequent photoionization of Ba.

Based on the appearance of the two ion clouds, it is apparent that KK produced a much smaller change in the ionospheric conductivity than did LL. This difference was undoubtedly related to the influence of the much higher electric field and faster cloud motion in KK. The I^- ion cloud was significantly more coupled to the neutrals than KK. Table 5 reports the estimated values of the coupling parameter η. From these values, the inferred ratio, α, of the field-line integrated Pedersen conductivity of the cloud, Σ_p^c, to the integrated conductivity of the ambient ionosphere, Σ_p^a, can be obtained.

Theoretically, the parameter $\zeta = 1 - \eta$ is a monotonically decreasing function of α. Figure 5 compares model calculations of this dependence with measurements. The middle curve (dot-dash) is $(1-\alpha/2)^{-1}$. The data were obtained primarily during

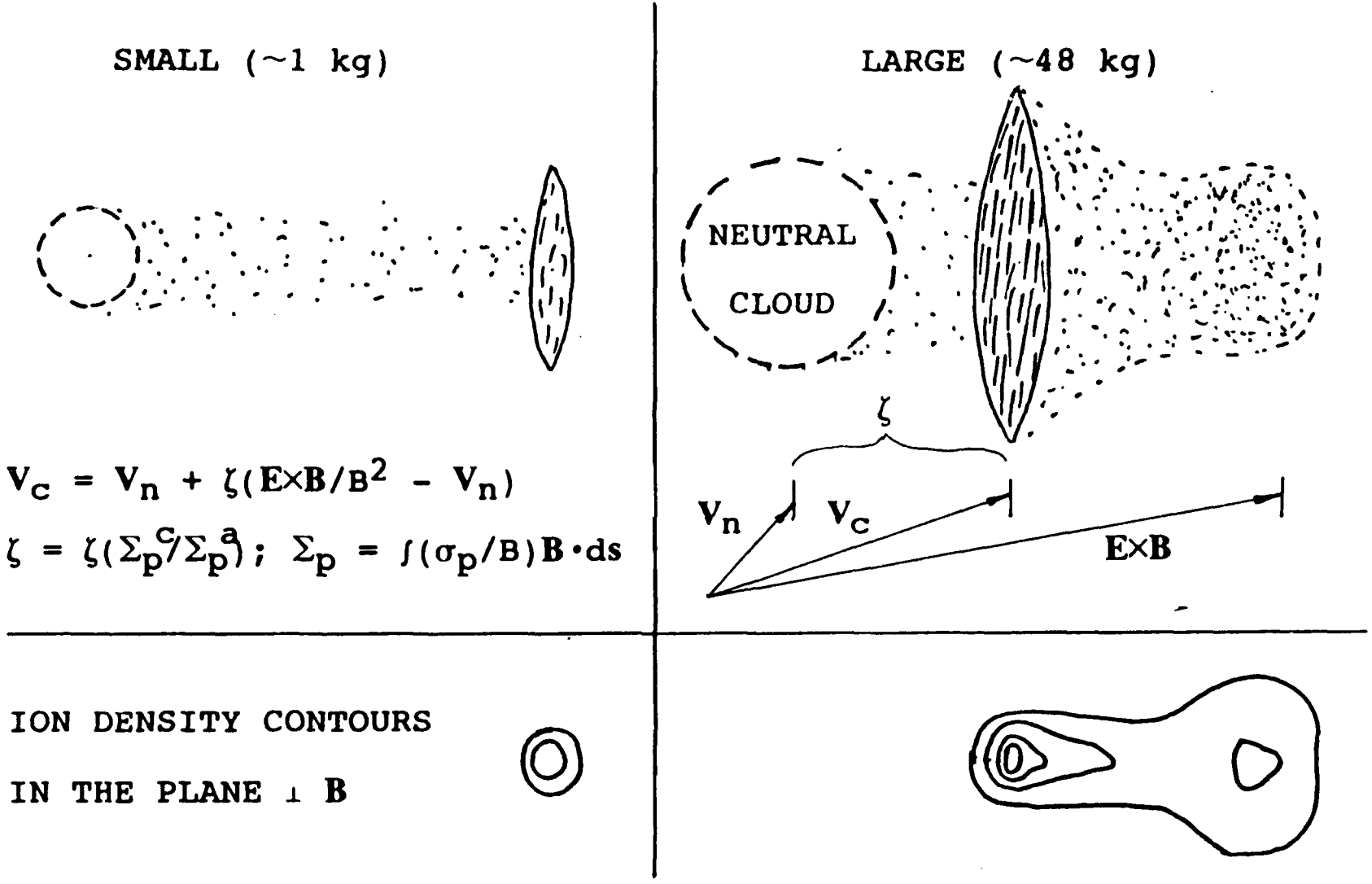

Figure 4. Sketches of barium ion cloud appearance for low-conductivity (small) and high-conductivity (large) clouds.

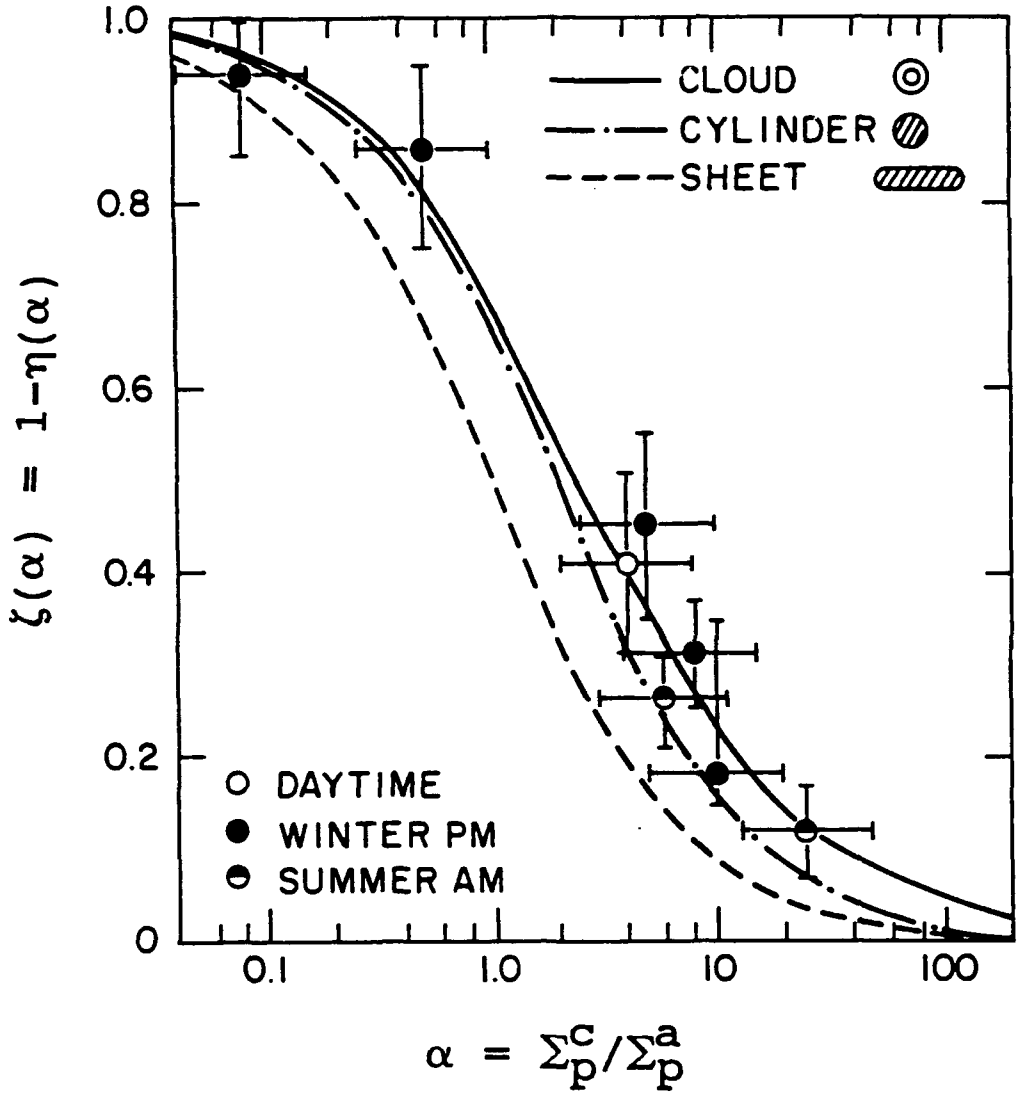

Figure 5. Coupling parameter ζ as a function of α.

SECEDE I and II. The solid curve appears to match the data better and was used to obtain the inferred conductivity ratios reported in the Table 5.

The Midnight Sky experience produced ion clouds with velocities both significantly slower and faster than was desired. If the experiment were to be repeated, it is imperative that at least a dry run and a wet run be carried out with all participants, systems, and links exercised. The mission would not have been successful had a launch occurred on the first opportunity. Instead, the first couple of scrubbed missions provided practice sessions. Establishment of the communication links and the expected mode of communication is important. This experience confirmed that the decision to take tracking data at regular preset intervals was a good one.

SECTION 3

LIST OF REFERENCES

1. Norman J. F. Chang, "PLACES TV-Track, Ionosonde, and Magnetometer Operations", DNA 5806F, SRI International, Menlo Park, California (June 1981).

2. Larry R. Rollstin and Fred V. Wyatt, "Real-Time Tracking and Targeting Computations and Rocket Vehicle Aeroballistics for the PLACES Ionospheric Plasma Test Series", SAND81-2091, Sandia National Laboratories, Albuquerque, New Mexico (February 1982).

3. Dan R. McDaniel, Compiler, "Proceedings of the PLACES Preliminary Data Review Meeting, 20 and 21 May 1981," DNA 5848P, SRI International, Menlo Park, California (July 1981).

4. L. R. Rollstin, "Rocket Operations" in Ref. 3, p. 189.

5. W. P. Boquist, "Ground Optics Photographic Measurements" in Ref. 3, p. 135.

6. Lewis M. Linson, "Status of Theoretical Understanding of Barium-Ion-Cloud Phenomenology," in Proceedings of the SECEDE II Final Data Review Meeting, p. 17, RADC-TR-72-153, Vol.II, Stanford Research Institute, Menlo Park, California (May 1972).

7. Lewis M. Linson, "Theory of Ion Cloud Dynamics and Morphology," in Analysis of Barium Clouds, Chapter 5, p. 106, RADC-TR-72-336, Vol. 1, Avco Everett Research Laboratory, Everett, Massachusetts, (October 1972).

8. Lewis M. Linson and David C. Baxter, "Ion Cloud Modeling", DNA 4455F, Science Applications, Inc., La Jolla, California, (November, 1977).

9. G. Haerendel, R. Lust, and E. Rieger, "Motion of Artificial Ion Clouds in the Upper Atmosphere", Planet Space Sci., 15, 1, 1967.

10. L. M. Linson, "Motion of Barium Ion Clouds," in Analysis of Barium Ion Clouds, RADC TR-72-103, Vol. I, p.39, Avco Everett Research Laboratory, Everett, Massachusetts, (January 1972).

11. L. M. Linson, "Effect of Conjugate Ionosphere and Shape on the Motion of Barium Ion Clouds," Trans., Am. Geophys. Union, 52, 880, 1971.

12. C. S. Stokes, C. T. Davey, and P. D. Zavitsanos, "Payload Description Document, Barium Vapor Release, Poker Flat Research Range, Alaska," Prepared for Geophysical Institute, University of Alaska, Fairbanks, Alaska, (March 1981).

13. P. D. Zavitsanos, F. N. Alyea, and J. A. Golden, "Redefinition and Improvement of Metal Vapor Release Technology," RADC-TR-77-269, General Electric Company/RESD, Philadelphia, Pennsylvania, (August 1977).

14. L. M. Linson and D. C. Baxter, "Gas Release and Conductivity Modification Studies," SAI02379-713LJ, LAPS-51, Science Applications, Inc., La Jolla, California, (May 1979).

DISTRIBUTION LIST

DNA-TR-89-55

DEPARTMENT OF DEFENSE

DEFENSE INTELLIGENCE AGENCY
ATTN: DB-6

DEFENSE NUCLEAR AGENCY
ATTN: PRPD R YOHO
3 CYS ATTN: RAAE K SCHWARTZ
ATTN: RAAE D RIGGIN
2 CYS ATTN: TITL

DEFENSE NUCLEAR AGENCY
2 CYS ATTN: FCTT W SUMMA
ATTN: TDNM

DEFENSE TECHNICAL INFORMATION CENTER
2 CYS ATTN: DTIC/FDAB

STRATEGIC DEFENSE INITIATIVE ORGANIZATION
ATTN: EN
ATTN: EN LTC C JOHNSON
ATTN: TDW
ATTN: TN DR M GRIFFIN

DEPARTMENT OF THE NAVY

NAVAL RESEARCH LABORATORY
ATTN: CODE 4780 B RIPIN
ATTN: CODE 4780 DR P BERNHARDT
ATTN: CODE 4780 J HUBA
ATTN: JACOB GRUN

DEPARTMENT OF THE AIR FORCE

AIR FORCE GEOPHYSICS LABORATORY
ATTN: LAILA DZELZKALNS
ATTN: OP W BLUMBERG

DEPARTMENT OF ENERGY

EG&G, INC.
ATTN: D WRIGHT

LOS ALAMOS NATIONAL LABORATORY
ATTN: R W WHITAKER

SANDIA NATIONAL LABORATORIES
ATTN: TECH LIB 3141

DEPARTMENT OF DEFENSE CONTRACTORS

AEROSPACE CORP
ATTN: BRIAN PURCELL
ATTN: C CREWS
ATTN: C RICE
ATTN: DR J M STRAUS
ATTN: G LIGHT
ATTN: M ROLENZ

BDM INTERNATIONAL INC
ATTN: W LARRY JOHNSON

BERKELEY RSCH ASSOCIATES, INC
ATTN: C PRETTIE
ATTN: J WORKMAN
ATTN: N T GLADD
ATTN: S BRECHT

CORNELL UNIVERSITY
ATTN: D FARLEY JR
ATTN: M KELLY

GENERAL RESEARCH CORP INC
ATTN: J EOLL

INSTITUTE FOR DEFENSE ANALYSES
ATTN: E BAUER
ATTN: H WOLFHARD

JAYCOR
ATTN: A GLASSMAN
ATTN: J SPERLING

JOHNS HOPKINS UNIVERSITY
ATTN: C MENG
ATTN: H G TORNATORE
ATTN: J D PHILLIPS
ATTN: R STOKES

KAMAN SCIENCES CORP
ATTN: DASIAC
ATTN: E CONRAD
ATTN: G DITTBERNER

KAMAN SCIENCES CORPORATION
ATTN: B GAMBILL
ATTN: DASIAC
ATTN: R RUTHERFORD

METATECH CORPORATION
ATTN: W RADASKY

MISSION RESEARCH CORP
ATTN: J KENNEALY
ATTN: R ARMSTRONG
ATTN: S DOWNER
ATTN: W WHITE

MISSION RESEARCH CORP
ATTN: R L BOGUSCH

MISSION RESEARCH CORP
ATTN: DAVE GUICE

MISSION RESEARCH CORP
ATTN: B R MILNER
ATTN: D KNEPP
ATTN: D LANDMAN
ATTN: F FAJEN
ATTN: F GUIGLIANO
ATTN: G MCCARTOR
ATTN: K COSNER
ATTN: M FIRESTONE
ATTN: R BIGONI
ATTN: R DANA
ATTN: R HENDRICK
ATTN: R KILB
ATTN: S GUTSCHE
ATTN: TECH LIBRARY

PACIFIC-SIERRA RESEARCH CORP
ATTN: E FIELD JR
ATTN: H BRODE

PHOTOMETRICS, INC
ATTN: I L KOFSKY

PHYSICAL RESEARCH INC
ATTN: W SHIH

PHYSICAL RESEARCH INC
ATTN: H FITZ

PHYSICAL RESEARCH, INC
ATTN: R DELIBERIS
ATTN: T STEPHENS

PHYSICAL RESEARCH, INC
ATTN: J DEVORE
ATTN: J THOMPSON
ATTN: W SCHLUETER

SCIENCE APPLICATIONS INTL CORP
2 CYS ATTN: L LINSON

SRI INTERNATIONAL
ATTN: W CHESNUT
ATTN: W JAYE

STEWART RADIANCE LABORATORY
ATTN: R HUPPI

TOYON RESEARCH CORP
ATTN: J ISE

UTAH STATE UNIVERSITY
ATTN: K BAKER
ATTN: L JENSEN

VISIDYNE, INC
ATTN: J CARPENTER

DIRECTORY OF OTHER

BOSTON UNIVERSITY
ATTN: MICHAEL MENDILLO